A two-dimensional geostatistic method to simulate the precision of abundance estimates

Alf Harbitz and Michaela Aschan

Abstract: In this paper, we outline a geostatistic method to simulate the relative precision (coefficient of variation, CV) of total abundance estimates of one species in a predetermined, stratified area when it is appropriate to treat the observations within each stratum as realizations of a second-order homogenous and ergodic random process. To model the spatial correlations, a variogram is fitted to normal-transformed values of the original observations. Based on the variogram and its corresponding covariance matrix, extensive simulations on a fine grid that includes the sample locations provide random realizations of the process. The normal values are back-transformed to original observation space by nonparametric reversed bootstrap, as well as by a parametric Weibull approach. The method is applied to a total of 1069 shrimp (*Pandalus borealis*) abundance observations from 11 annual surveys in the Barents Sea (1992–2002) where a 20 nautical mile sampling grid has been applied. On average, the CV was estimated to be 6.4% for the applied regular grid when the simulations were conditional on the observations, compared with 8.1% when the sampling locations within each of the six strata were random.

Résumé : On trouvera ici la description d'une méthode géostatistique pour simuler la précision relative (coefficient de variation, CV) des estimations d'abondance totale d'une espèce dans une aire prédéterminée et stratifiée, lorsqu'il est approprié de traiter les observations dans chacune des strates comme les résultats d'un processus aléatoire de second degré homogène et ergodique. Afin de modéliser les corrélations spatiales, nous ajustons un variogramme aux valeurs normalisées des observations originales. Des simulations répétées, basées sur le variogramme et sa matrice de covariance correspondante et faites sur une grille fine qui comprend les stations d'échantillonnage, fournissent des résultats aléatoires du processus. Les valeurs normalisées sont retransformées dans l'espace original d'observation au moyen d'un bootstrap non paramétrique inversé, ainsi qu'au moyen d'une approche paramétrique de Weibull. La méthode est utilisée sur un total de 1069 observations d'abondance de crevettes (*Pandalus borealis*) provenant de 11 inventaires dans la mer de Barents (1992–2002) qui emploient une grille d'échantillonnage de 20 milles marins. En moyenne, le CV est estimé à 6,4 % pour la grille utilisée lorsque les simulations sont dépendantes des observations, alors qu'il est de 8,1 % lorsque les sites d'échantillonnage dans chacune des six strates sont aléatoires.

[Traduit par la Rédaction]

Introduction

In classical sampling theory, random sampling locations are often advocated in order to get design-unbiased estimates of abundance (Cochran 1977). In these cases, the population of all possible sample outcomes in terms of abundance observations is considered fixed, while the randomness is included in the sampling design. In the so-called model approach (Thompson 1992; Thompson and Seber 1996) applied in this paper, the opposite is true. Using this approach, sampling sites are fixed and the sample outcomes are stochastic. If the sampled abundance observations can be considered a random sample from the population distribution of all possible sample outcomes, then an unbiased abundance estimate can be provided with respect to the population distribution.

There is no general rule saying that one of the above approaches is superior to the other. The random sampling approach is the most robust one in the sense that there is no need to model either the population distribution of possible abundance observations or spatial correlations. Another advantage is that the minimum sailing distance tends to be shorter than for regular sampling (Beardwood et al. 1959; Christofides and Eilon 1969). It is also clear that the model approach must assume some kind of randomness in the spatial distribution of the abundance to provide unbiased abundance estimates. On the other hand, when spatial correlations between observations are present and the spatial structure can be appropriately modelled, more precise abundance estimates may be obtained with a regular sampling design than by random location sampling (Cochran 1977; Rivoirard et al. 2000). Another argument in favour of regular sampling is that the tidy

Received 13 March 2002. Accepted 19 October 2003. Published on the NRC Research Press Web site at http://cjfas.nrc.ca on 22 December 2003.
J16806

A. Harbitz[1] and M. Aschan. Institute of Marine Research, Havforskningsinstituttet, Sykehusvegen 23, PB 9404, 9294 Tromsø, Norway.

[1]Corresponding author (e-mail: alf.harbitz@imr.no).

 doi: 10.1139/F03-134

handling of the samples could be very complicated with succeeding stations close to each other (Harbitz et al. 1998).

In this paper, the abundance observations during a survey are considered as realizations of a second-order homogenous random process, which is in accordance with the intrinsic hypothesis in geostatistics (Rivoirard et al. 2000). This means that a possible spatial correlation between two observations is dependent on the distance between their locations only. This is a situation that is realistic for many surveys but is especially true in the open sea (Harbitz and Lindstrøm 2001). The term "homogenous process" was deliberately chosen over the more traditional term "stationary process". This is partly because the focus is on the spatial properties of the process and partly because the process is a spatial–temporal process where different terms in space and time are useful. The term "stationary" is, in our opinion, a more natural term to use with respect to time.

Even if a regular grid under the homogeneity assumption provides classical unbiased abundance estimators, it is more difficult to obtain unbiased variance estimators due to the possible spatial correlations between the samples. To examine if such correlations exist and to take this into account in the variance, geostatistics has proven to be an appropriate tool. During the last decade, there has been an increased focus on spatial statistics within marine resource abundance estimation (Petitgas 1993; Rivoirard et al. 2000).

In this paper, a general two-dimensional simulation method is outlined that provides good estimates of abundance estimator precision, taking the spatial correlation appropriately into account. A major feature of this approach is that there is no need to establish a good model for the spatial correlations in original observation space. It is sufficient to have a good model in normal-transformed space, which in practice is much easier to obtain.

Though many of the different elements of the method are not new, the composition and focus differ from earlier work (e.g., Petitgas 1993; Kern and Coyle 2000). As an example, the method includes a nonparametric approach in which the empirical abundance distribution can be used in the back-transformation from normal space to abundance space (reversed bootstrap; Harbitz and Lindstrøm 2001). In addition, it is straightforward to implement irregular contours that enclose the study area.

An important element of the method is that it accounts for the fact that the expected sampling variance in cases in which density observations are positively correlated will be smaller than the variance in the process distribution that generates random realizations of the process. This difference is due to a finite study area and is important when the correlation length, i.e., the distance between two observations beyond which the spatial correlation disappears, is not negligible compared with the extension of the area.

The method can, in principle, be applied to any sampling design and so is useful for comparing different sampling designs. A major goal of the present study is to offer an easily applied and useful supplement to the geostatistic tool kit for estimating the precision of abundance estimates.

Materials and methods

Notations are given in Appendix A and a detailed chart of the simulation procedure is given in Appendix B.

The Barents Sea shrimp data

The Barents Sea is delineated by the coastline of northern Norway and Russia in the south, by Bear Island and Spitzbergen towards the west, and by Novaja Zemlja and Frans Josef Land at the east and the north (Fig. 1). It is a relatively shallow shelf sea with a mean depth of 230 m, covering approximately 1.4 million km^2. The Atlantic water from the south and the colder, less saline Arctic water from the north meet in the Polar Front. During winter, the Arctic water is covered with ice, but most of the Barents Sea is ice-free during summer (Loeng 1991). The shrimp stock is distributed throughout the area at depths deeper than 150 m. Norway has conducted annual shrimp surveys in the Barents Sea in April–May since 1982. The study area is divided into six strata (A–F) and covers approximately 50 000 nautical miles^2 (n.mi.^{2}) (Fig. 1). A Campelen 1800 survey trawl was towed at 3 knots for 20 min, resulting in a tow distance of 1 n.mi. Since 1992, a 20 n.mi. regular grid has been used to locate trawl stations (Fig. 1), and data from 1992–2002 are used in this study. The actual trawl stations in 1992 (shown as solid circles in Fig. 1) are close to the idealized nodes in the grid. In 1996, a 10 n.mi. sampling grid was used in the area where shrimp were most abundant (stratum E) to study the abundance variation on a finer scale than 20 n.mi. Stratum E had the greatest abundance of shrimp (*Pandalus borealis*), but it was also the stratum with the most difficulties caused by ice (Fig. 2). The location of the fine 2 n.mi. simulation grid nodes applied in this stratum are shown as dots, along with the actual sampling sites (solid circles) in 1996 approximated to the nearest 2 n.mi. grid node. For the other strata, a 4 n.mi. simulation grid was chosen.

A total of 1069 trawl stations with distinct sampling locations for each survey are included in the analyses of the coefficient of variation. In addition, in several surveys the same locations have been repeatedly trawled within a few hours. These observations provided a total of 115 different within-survey observation pairs. Aschan and Sunnanå (1997) gave a detailed description of the surveys.

The abundance and its estimator

Let b denote density, e.g., in tonnes·n.mi.$^{-2}$. Density, $b = b(\mathbf{x},t)$, is generally a function of time, t, and horizontal location in space, $\mathbf{x} = (x, y)$. For simplicity, the vertical component is omitted here. The abundance (biomass or number) to be estimated, B, is then

$$(1) \qquad B(t) = \mu(t)A = \int_{\Omega} b(\mathbf{x})\mathrm{d}(\mathbf{x})$$

where A is the area of the predetermined region Ω of interest. Further, μ is the average density and $\mathrm{d}\mathbf{x} = \mathrm{d}x\mathrm{d}y$. For simplicity, only one stratum is considered initially; the extension to m nonoverlapping strata will be discussed later. It is assumed that B is varying slowly in time on a time scale corresponding to the duration Δt of a survey. Because the area is assumed to be known, estimation of B is synonymous with estimation of μ.

Let $\mathbf{b}_s = (b_1, \ldots, b_n)$ denote a density sample vector consisting of n density observations at the location $\mathbf{x}_s = (\mathbf{x}_{s1}, \ldots, \mathbf{x}_{sn})$, where subscript "s" is used as an abbreviation for sample observation. The classical abundance estimator, $\hat{B}$, for the abundance is now

Fig. 1. The location of the Barents Sea shrimp (*Pandalus borealis*) study area, along with its six main strata A–E. Idealized regular 20 nautical miles (n.mi.) sampling grid nodes are indicated by plus signs (+), and the actual sampling sites in 1992 are indicated by solid circles (●).

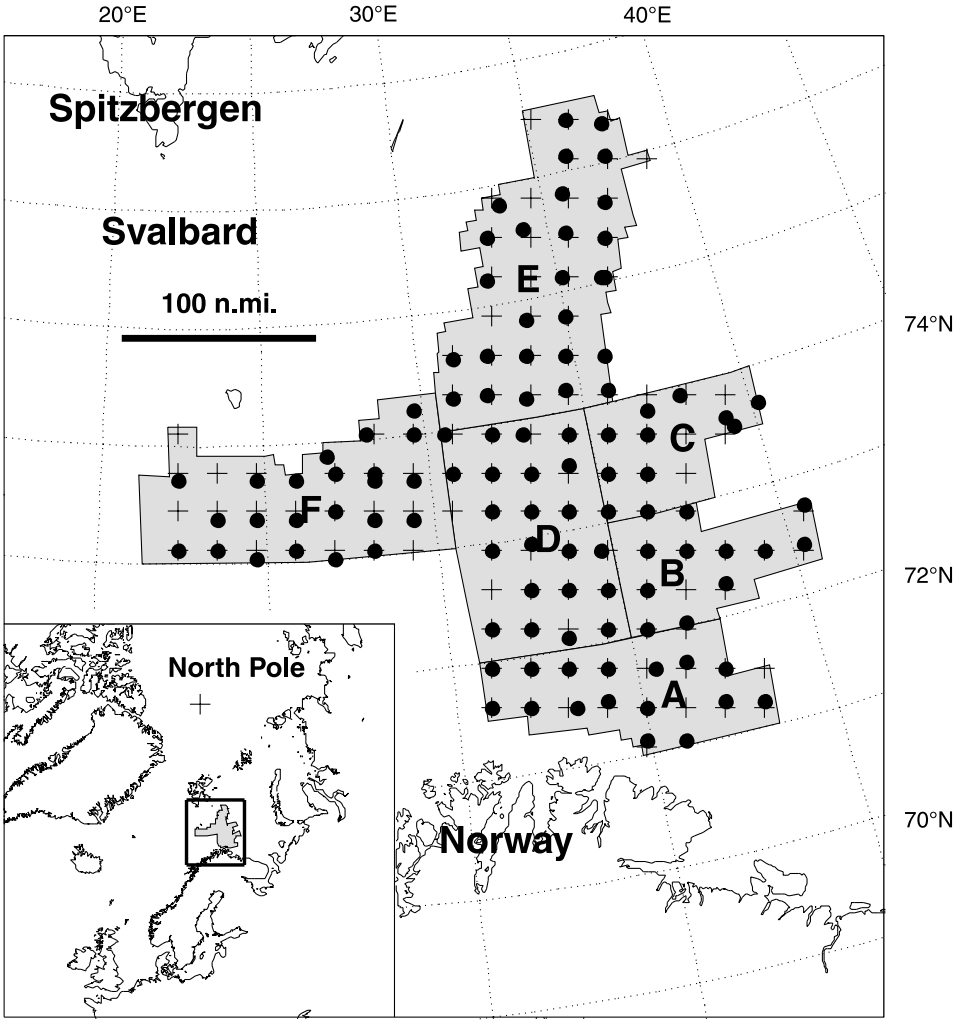

$$\hat{B} = \frac{1}{q}\left(\frac{1}{n}\sum_{j=1}^{n} b_j\right)A = \bar{b}A/q \qquad (2)$$

where a bar over a variable denotes arithmetic average and q is catchability. For simplicity, q is assumed to be constant; then q disappears from the CV expressions to follow and will from now on be set equal to one. In a fixed-population approach, the estimator above is unbiased under a randomized design, e.g., when the n observation locations are chosen randomly. Under the intrinsic geostatistic hypothesis, which is the approach used in this paper, the estimator is unbiased under any sampling design that is not dependent on the observation variable, e.g., a regular sampling grid (Petitgas 1993). The term unbiased, as used in this intrinsic geostatistic context, implies that $E(\hat{\mu}\,|\mu) = \mu$ (conditional unbiasedness), where $\hat{\mu} = \bar{b}$ and the expectation is taken with regard to the distribution of all possible realizations of the process providing μ and $\hat{\mu}$.

If all b_js are uncorrelated, the following estimator, $\hat{\sigma}^2_{\hat{B}}$, will be an unbiased variance estimator for $\sigma^2_{\hat{B}} = \mathrm{var}(\hat{B})$, independent of population distribution:

$$\hat{\sigma}^2_{\hat{B}} = S^2A^2/n \qquad (3)$$

where $S^2 = (1/(n-1))\sum_{j=1}^{n}(b_j - \bar{b})^2$ is the sample variance, which in this case is an unbiased estimator for $\sigma^2 = \mathrm{var}(b_j)$. A reasonable (though in general biased) estimator $\hat{\mathrm{CV}}_0$ for the coefficient of variation $\mathrm{CV}_0 = \sigma_{\hat{B}}/B$ is in this case

$$\hat{\mathrm{CV}}_0 = \frac{\sqrt{\hat{\sigma}^2_{\hat{B}}}}{\hat{B}} \qquad (4)$$

If spatial correlations between observations are present, the variance estimator in eq. 3 is biased (unless the sample locations are random). A key focus in this paper is to provide a CV estimator with negligible bias that takes such spatial correlations into account, assuming that it is reasonable to treat the set of possible density samples in a survey as a realization of a second-order homogenous random process. The geostatistic variogram is applied as the structural tool, and the corresponding covariance is applied for simulations of random realizations of the process.

Fig. 2. The most abundant shrimp area, Hopen area (stratum E), with the fine 2 nautical mile simulation grid nodes indicated by dots. The actual sampling sites in 1996 approximated to the nearest simulation grid nodes are indicated by solid circles (●).

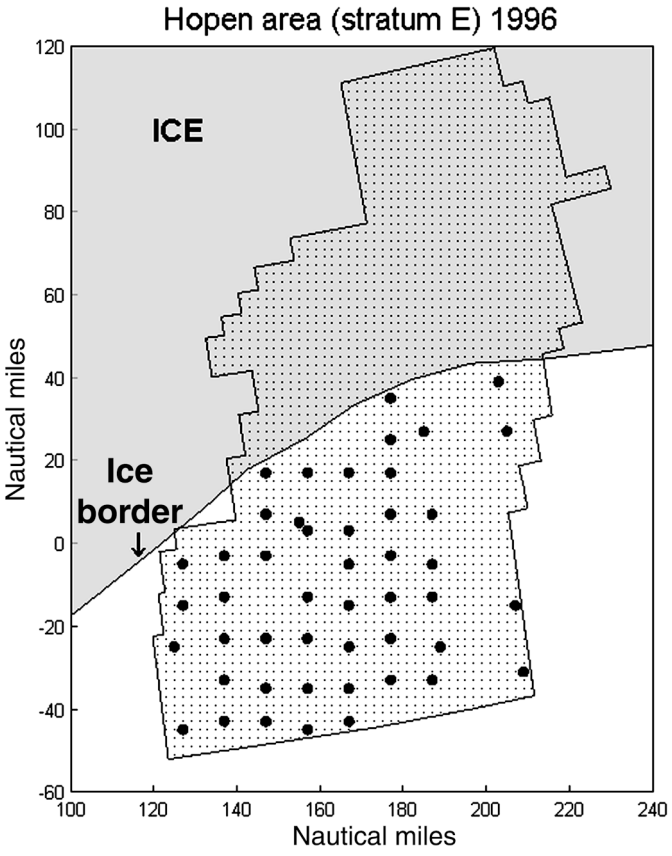

Variogram and covariance

The realization $\mathbf{b}_s = (b_1, \ldots, b_n)$ of n density observations at a particular time, t, is considered a realization of a second-order homogenous random process, b, with properties

$$(5) \qquad Eb(\mathbf{x} + \mathbf{h}) = Eb(\mathbf{x})$$
$$\operatorname{cov}(b(\mathbf{x}), b(\mathbf{x} + \mathbf{h})) = \mathbf{C}_b(\mathbf{h})$$

The expectation and the covariance are with respect to all possible realizations of the process, and $\mathbf{C}_b$ denotes the covariance matrix of the process.

To get the necessary link between statistics of different realizations and the statistics in space for a given realisation (where we have data), we assume that the process is ergodic (Cressie 1993). In other words, averaging over realizations (ensemble average) at any given location in space is equivalent to averaging in space over an infinite area for any realization.

The sample and process distributions

However, because the study area is limited, the statistics of the sampled densities within the area for a given realization will differ from the infinite situation. To distinguish the finite and infinite cases, the terms sample and process (population) distributions will be distinguished. The sample distribution is the empirical distribution of the real density observations, or a fitted parametric distribution. The process distribution is the distribution of a single density observation drawn randomly at any location from the distribution of possible process realizations and is the appropriate one to be used in the density simulations (to which we return later). Because of the assumption of ergodicity, the process distribution is synonymous with the sample distribution of an infinite number of observations evenly spread over an infinite area.

The sample distribution will depend on the sampling design and will tend to be less dispersed (possess a smaller variance) than the process distribution resulting from a finite study area (Fig. 3). For a fixed area, the similarities between the two distributions will increase with a decreasing range (correlation length) and an increasing number of evenly distributed sampling locations. An important feature of the simulation method is the ability to account for the difference between the sample and process distributions with regard to the variance.

Variogram, covariance, and normal transformation

The variogram in observation space, $\gamma_b(\mathbf{h})$, and its correspondence with the covariance matrix, $\mathbf{C}_b(\mathbf{h})$, are

$$(6) \qquad \gamma_b(\mathbf{h}) = \tfrac{1}{2}\operatorname{var}(b(\mathbf{x} + \mathbf{h}) - b(\mathbf{x})) = \mathbf{C}_b(\mathbf{0}) - \mathbf{C}_b(\mathbf{h})$$

where the latter equality follows from the homogeneity assumptions given by eq. 5 and $\mathbf{C}_b(\mathbf{0})$ equals the variance in the process distribution. For convenience, only isotropic variograms will be considered; in which case, the variogram becomes a one-dimensional function of the lag, $h = |\mathbf{h}|$.

There exist several theoretical models for the variogram (Rivoirard et al. 2000). To be considered, the candidate model must be consistent with a positive definite covariance matrix, $\mathbf{C}_b$. Before a model is chosen, an empirical variogram should be examined. Because of the generally skewed population distributions of abundance observations, it is recommended (Petitgas 1993) that the observations be normalized before the empirical variogram is calculated. This is partly to examine if a structure exists and, if so, to stabilize the variogram. Nonparametrically, the Φ transformation can be applied, transforming the original observations $b_1, \ldots, b_n$ to quantiles $z_1, \ldots, z_n$ in the standard normal $N(0,1)$ distribution based on the ranks of the original observations (Petitgas 1993):

$$(7) \qquad z_j = k\Phi^{-1}(\operatorname{rank}(b_j)/(n + 1)), \quad j = 1, \ldots, n$$

where k is a correction factor (close to one) to obtain a sample variance of the z values equal to one and independent of n. The corresponding normalized variogram is denoted $\gamma_z(h)$, and the corresponding covariance matrix is $\mathbf{C}_z(h) = 1 - \gamma_z(h)$.

A widely used variogram model made of a nugget effect and a spherical function was chosen to fit the empirical shrimp variograms:

$$(8) \qquad \gamma_Z(h) = \begin{cases} \mathrm{NU} + (\mathrm{SI} - \mathrm{NU})(1.5(h/r) - 0.5(h/r)^3), & 0 \le h \le r \\ \mathrm{SI}, & h > r \end{cases}$$

Fig. 3. Illustration of the difference between the process distribution and the less dispersed sampling distribution in a realization of a one-dimensional (1D), 2nd-order homogenous and ergodic random process with NU = 0.4 and r = 75. The broken line illustrates a more extensive part of the "infinite" process realization than the solid line, which is limited by the sampling domain.

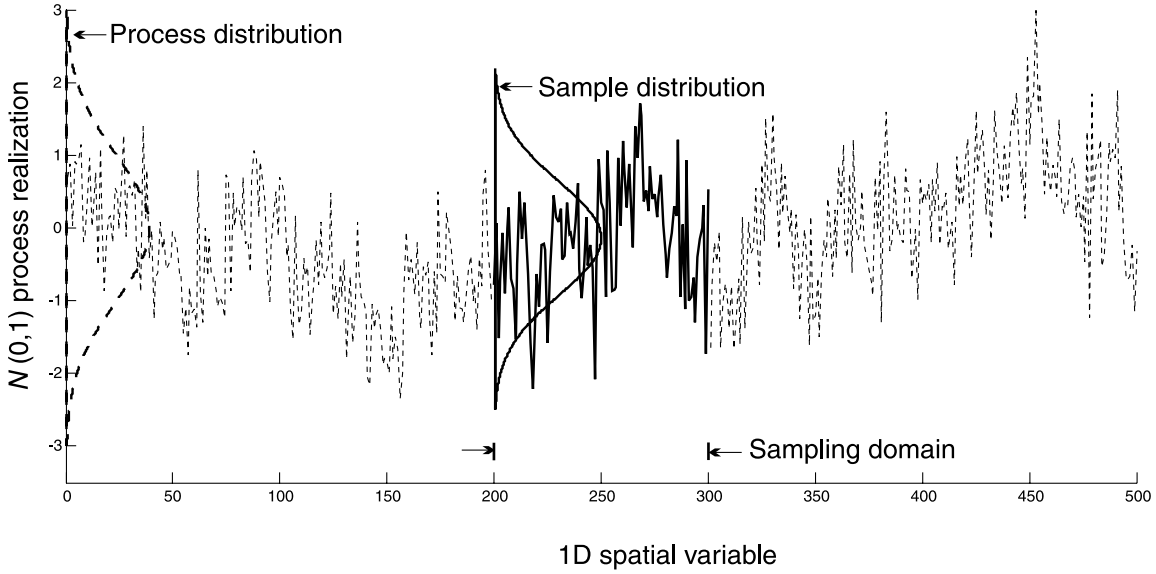

The three parameters are NU (expressing the nugget effect), SI = $\mathbf{C}_z(0)$ (the asymptotic value of the variogram (the sill)), and r, the range beyond which the spatial correlation disappears. The critical parameter is NU, which expresses the variance contribution due to random (nonstructural) variation as well as local spatial variations on a much finer spatial scale than what is possible or practical to detect at the sampling scale.

To get a first visual impression of the empirical variogram $\hat{\gamma}_Z(h)$, this is often done by averaging within equidistant distance bins:

(9)
$$\hat{\gamma}_Z(h) = \frac{1}{2n_h}\sum_{j,k}(z_j - z_k)^2, \qquad h_{jk} \in \left[h - \frac{dh}{2}, h + \frac{dh}{2}\right],$$
$$h = dh, 2dh, \ldots, n_{\text{lag}}dh$$

where the lag resolution, dh, may correspond to the average distance between two adjacent observations. The sum is over all n_h pairs of observations with distance h_{jk} within the interval given by the brackets, and h is divided into equidistant steps $dh, 2dh, \ldots, n_{\text{lag}}dh$. The shape of the empirical variogram is an important first validation check of the homogeneity assumption, where the absence of an apparent horizontal asymptote (possibly superimposed by cyclic oscillations) is an indication of nonhomogenous conditions.

Note that there is generally no trivial correspondence between the variogram γ_z in normal-transformed space and the variogram γ_b in original observation space, though transformation formulas exist for special cases (Rivoirard et al. 2000). Even if the same model applies in both cases (e.g., the nugget + spherical model), the NU-to-SI ratio (NU:SI) will, in general, differ. A great advantage of the simulation approach is that a good variogram model in normal-transformed space is sufficient, precluding the need to know the variogram in original observation space.

Estimation of variogram parameters for a regular sampling grid

For a regular sampling grid, there are a limited finite number of distinct h values with rather many observations at many of the discrete hs. By using this, the need for smoothing in eq. 9 is avoided, and a better basis is obtained for the estimation of the variogram parameters. Let h_d, γ_d and n_d denote the lag, the variogram, and the number of observations with a distance h_d apart, respectively, by this discrete approach, where d = 1, …, n_d, and n_d denotes the number of discrete lags. The parameters NU, SI, and r can be estimated by minimizing a sum of (weighted) squares of terms that reflect the differences between the theoretical and empirical variograms at each lag. The following sum appeared to give better results for the shrimp data than the more common sums given in the theory chapter in Rivoirard et al. (2000):

(10) $$Q = \sum_{d=1}^{n_r} \ln^2(\hat{\gamma}_d(h_d)/\gamma_d(h_d))n_d$$

where $\hat{\gamma}_d$ is calculated analogous to eq. 9, and n_r is equal to the number of distinct h_d values less than or equal to r, or a slightly larger value based on a rough estimate of r from the variogram provided by eq. 9. The reason for this restriction on n_r is that NU is considered to be the most important parameter, and its estimator should not be influenced by variogram values at lags beyond the range r. The rational for using the logarithm of the variogram values is that the coefficient of variation of $(z(\mathbf{x} + \mathbf{h}) - z(\mathbf{x}))^2$ at each lag $h_d = |\mathbf{h}|$ is constant, thus each term in the sum is expected to have approximately the same variance if the variogram model is appropriate.

Studying the summation terms before they are squared as a function of h_d is considered a fair model validation check, where independence, homoscedasticity (constant variance), and absence of trends are model-supporting properties. Note, however, that many of the variables contributing to each

term in the sum are dependent, which complicates the challenge of finding an optimal construction of the square sum to be minimized. The properties (accuracy, precision, and covariation) of the estimators determined by this approach can be assessed by Monte Carlo simulation as described later.

An important validation technique (Chilès and Delfiner 1999) is to analyze scatterplots for the pairs of z values at locations providing the same lag, h. These should be elliptically shaped with a correlation coefficient similar to the covariance, $\mathbf{C}_z(h)$, in normal-transformed space calculated from the variogram model and in accordance with a binormal distribution.

The expectation of the sample variance equals the mean of the empirical variogram values for positive lags, i.e., $ES^2 = \overline{\gamma}_+$. Thus for evenly distributed sampling locations (regular or random) and a small range compared with the extension of the area, the estimated SI should be close to one under the assumptions made.

Monte Carlo simulation

The simulation procedures are first outlined for one area and for nonconditional simulations, i.e., simulations that are not dependent on the actual density observations at the sampling sites. To distinguish nonconditional from conditional simulations introduced later, the subscripts "nc" and "c" will be used, respectively. At the end of the section, how to treat a study area consisting of m adjacent strata is outlined.

The simulation grid and random N*(0,1) realizations*

A variogram model consistent with an isotropic and homogenous process of second order is synonymous with a one-to-one correspondence between the covariance of normalized variables at two different locations and the variogram

$$(11)\quad c_{jk} = \mathrm{cov}(z_j, z_k) = \begin{cases} 1-\gamma_Z(h_{jk}), & j \neq k \\ 1, & j = k \end{cases}$$

where $h_{jk} = |\mathbf{x}_j - \mathbf{x}_k|$ denotes the distance between the locations $\mathbf{x}_j$ and $\mathbf{x}_k$.

Now define a fine, regular simulation grid, with N grid nodes at $\mathbf{x}_g = (\mathbf{x}_{g1}, \ldots, \mathbf{x}_{gN})$ located so that a minimum distance between the sampling sites and the nearest nodes in the simulation grid is obtained. These approximate sampling locations will be denoted sampling nodes. The resolution in the simulation grid (distance between adjacent nodes) should be so fine that a negligible difference between the true density μ and the average of the N densities at the grid nodes is obtained.

Let $\mathbf{C}(\mathbf{x}_g,\mathbf{x}_g) = \{c_{jk}\}$ denote the $N \times N$ grid covariance matrix found by using eq. 11 with $h_{jk} = |\mathbf{x}_{gj} - \mathbf{x}_{gk}|$, and let $\mathbf{D}$ denote a decomposition of $\mathbf{C}(\mathbf{x}_g,\mathbf{x}_g)$ so that $\mathbf{DD}^T = \mathbf{C}(\mathbf{x}_g,\mathbf{x}_g)$. A random realization vector of normalized densities at all nodes, $\mathbf{z}_{nc}(\mathbf{z}_g)$, with the appropriate spatial correlation structure can then be generated as follows:

$$(12)\quad \mathbf{z}_{nc}(\mathbf{x}_g) = \mathbf{D}\mathbf{z}_{iid},\ \mathbf{DD}^T = \mathbf{C}(\mathbf{x}_g,\mathbf{x}_g)$$

where superscript "T" denotes transpose, and $\mathbf{z}_{iid}$ is a $N \times 1$ vector of independent $N(0,1)$ variables. The simulation by eq. 12 is repeated n_{sim} times to obtain a sufficient number of random realizations. For the variogram in eq. 8, it is convenient to split the simulations into one structural part and one white-noise part as follows:

$$(13)\quad \mathbf{z}_{nc}(\mathbf{x}_g) = (1 - \mathrm{NU})^{1/2}\mathbf{D}_0\mathbf{z}_{iid,1} + (\mathrm{NU})^{1/2}\mathbf{z}_{iid,2}$$

where $\mathbf{D}_0\mathbf{D}_0^T = \mathbf{C}_0 = \mathbf{C}(\mathbf{x}_g,\mathbf{x}_g;\ \mathrm{NU} = 0,\ \mathrm{SI} = 1)$ and $\mathbf{z}_{iid,1}$ and $\mathbf{z}_{iid,2}$ are independent $N \times 1$ vectors of independent $N(0,1)$ variables. If, for example, different nugget values are to be used, $\mathbf{D}_0$ is the only decomposed matrix needed.

There are several candidates for $\mathbf{D}$, where a very fast numerical solution is to define $\mathbf{D}$ as a Cholesky decomposition of $\mathbf{C}$ (Ripley 1987). Note, however, that if the Cholesky factorization creates an upper-triangular matrix $\mathbf{D}$, not a lower-triangular matrix as defined by Ripley (1987), $\mathbf{D}$ in eq. 12 should be replaced by $\mathbf{D}^T$. This is the case in Matlab (The Mathworks, Inc., Natick, Mass.), the computer program used to provide the results in this paper. Another important precaution that should be considered with regard to a Cholesky decomposition is that a variety of numerical inaccuracies might occur if $\mathbf{D}$ is large, e.g., greater than 1000×1000 (Cressie 1993). An easy way to check this is to calculate $\mathbf{DD}^T$ after the decomposition and see if each element deviates from the corresponding element in the original $\mathbf{C}$ within the accuracy of the computer. In the Barents Sea application (returned to later), $\mathbf{D}$ is a 5035×5035 Cholesky decomposition matrix, and no numerical problems occurred. Other more robust (and slower) decomposition techniques are described by Chilès and Delfiner (1999, p. 465).

Conditional simulation

Conditional simulation in a geostatistic context is synonymous with simulations of random realizations of a process with the constraint that the simulations are conditional on the observed values at the sample locations (Cressie 1993; Chilès and Delfiner 1999). This is an appealing feature, because it intuitively takes peculiarities of the realization providing the observations into account better than nonconditional simulation. Mathematically, the multinormal distribution of $\mathbf{z}_g$, conditional on the normal-transformed observations $\mathbf{z}_s$, is the basis for the conditional simulations. This distribution, $f(\mathbf{x}_g|\mathbf{x}_s)$, was outlined based on standard multivariate calculations (Mardia et al. 1992), modelling the process as the sum of a pure spatial structure component and a white-noise (nugget) component. As a result, the following expressions were found for the conditional expectation $E(\mathbf{z}_g|\mathbf{z}_s)$ and covariance matrix $\mathbf{C}_c = E(\mathbf{z}_g\mathbf{z}_g^T|\mathbf{x}_s)$, where subscript c denotes conditional:

$$(14)\quad E(\mathbf{z}_g|\mathbf{z}_s) = (1 - \mathrm{NU})\mathbf{C}_0(\mathbf{x}_g,\mathbf{x}_s)\mathbf{C}(\mathbf{x}_s,\mathbf{x}_s)^{-1}\mathbf{z}_s$$

$$\mathbf{C}_c = E(\mathbf{z}_g\mathbf{z}_g^T|\mathbf{z}_s) = \mathbf{C}(\mathbf{x}_g,\mathbf{x}_g) - (1 - \mathrm{NU})^2 \times \mathbf{C}_0(\mathbf{x}_g,\mathbf{x}_s)\mathbf{C}(\mathbf{x}_s,\mathbf{x}_s)^{-1}\mathbf{C}_0(\mathbf{x}_s,\mathbf{x}_g)$$

Subscript 0 in the expressions above denotes, as before, that the actual matrix is calculated with NU = 0 and SI = 1. Note that the dimensions of the matrices above are given by the subscript on the $\mathbf{x}$s. As an example, $\mathbf{C}_0(\mathbf{x}_g,\mathbf{x}_s)$ is an $N \times n$ matrix where the elements are calculated as follows:

$$(15)\quad \mathbf{C}_0(\mathbf{x}_g,\mathbf{x}_s) = \{\mathrm{cov}_0(|\mathbf{x}_{gj} - \mathbf{x}_{sk}|)\},\quad j = 1,\ldots, N,\ k = 1,\ldots, n$$

where cov_0 denotes the covariance with NU = 0 and SI = 1.

Based on eq. 14, the following procedure can be used to generate random realizations of the process conditional on observations, $\mathbf{z}_c(\mathbf{x}_g) = z(\mathbf{x}_g|\mathbf{z}_s)$:

$$\mathbf{z}_c(\mathbf{x}_g) = (1 - \text{NU})\mathbf{C}_0(\mathbf{x}_g,\mathbf{x}_s)\mathbf{C}(\mathbf{x}_s,\mathbf{x}_s)^{-1}\mathbf{z}_s + \mathbf{D}_c\,\mathbf{z}_{\text{iid}} \quad (16)$$

where $\mathbf{D}_c$ is a decomposition of $\mathbf{C}_c$ (e.g., Cholesky), i.e., $\mathbf{C}_c = \mathbf{D}_c\mathbf{D}_c^{\mathrm{T}}$, and $\mathbf{z}_{\text{iid}}$ is a $N \times 1$ vector of iid $N(0,1)$ variables.

Parameter uncertainties

Based on the random realizations by using eq. 12 or eq. 13, the properties of variogram parameter estimators such as the least squares estimators defined by minimizing the square sum in eq. 10 can be estimated. In these simulations, the parameter estimates based on normal-transformed real data are used as true values except that SI is set equal to one, which is the appropriate value in the process distribution. Then the covariance matrix to be used in the simulations is established with elements defined by eq. 11. Note, however, that now only the n sampling nodes are used.

For each random realization at the sampling nodes, new estimates of the involved variogram parameters are estimated. The properties of the estimators are then assessed based on the simulated estimates. To obtain reasonable estimates of bias and variance, about 1000 simulations are sufficient for most practical situations. If the absolute value of the bias is considerably less than the standard deviation, the bias is normally considered to be negligible.

Backtransformation from N*(0,1) to biomass densities and estimation of scaling factor between standard deviations in sampling and process distributions*

The simulated normal variates at the sampling nodes can also be used to simulate the scaling factor needed to take account of the different dispersions in the process and sampling distributions. This can be done either based on the empirical sampling distribution, which is called reversed bootstrap (Harbitz et al. 2001), or by use of a fitted parametric distribution. First the cumulative $N(0,1)$ value Φ is calculated for each generated $N(0,1)$ value z. If a parametric cumulative sampling distribution, F, is applied, each z value is then back-transformed to a density b by the equation $b = F^{-1}(\Phi(z))$, where F^{-1} denotes the inverse cumulative distribution function. In the reversed bootstrap case, the Φ values are first made discrete by the formula $R = \text{int}(\Phi n) + 1$, where "int" rounds Φn to the nearest integer towards zero. The assigned observation value is then the observed density with rank equal to R. The rational for the bootstrap term in this context is that the empirical population distribution is used to mimic the true population distribution, which is a basis for bootstrap.

The sample distribution is now treated as the true process distribution, and the distribution of the back-transformed densities from the $N(0,1)$ realizations are treated as simulated sample distributions. This is analogous to the change of roles between an unknown parameter and its estimate from data when simulations are performed to examine the properties of the estimator. Because of the finite area effect, the average standard deviation, S_{MC}, of the simulated sample distributions should be less than the standard deviation, S, in the empirical sample distribution. In the CV expressions to follow, the lack of dispersion by applying the sample distribution to mimic the process distribution is taken into account by using S/S_{MC} as a scaling factor.

Estimation of precision

Let the true abundance density, μ, with estimator, $\hat{\mu}$, at the time of sampling correspond to one realization of the process. The challenge is to find an appropriate estimator for the CV of $\hat{\mu}$. Based on the previously described procedures, n_{sim} random realizations in $N(0,1)$ space are generated with one value in each simulation grid node. For each realization, the normal values are back-transformed to density values parametrically or nonparametrically as described before. The average based on simulations in each of the fine grid nodes, $\bar{b}_g$, is treated as the true density of that particular realization. The simulated density estimate is the average, $\bar{b}_s$, of the simulated values at the sampling nodes. An appropriate estimator for $\text{CV}(\hat{\mu})$ is then obtained as follows:

$$\hat{\text{CV}} = (S/S_{\text{MC}})\,\hat{\text{std}}(\bar{b}_s/\bar{b}_g) \quad (17)$$

where $\hat{\text{std}}$ is the standard deviation of the n_{sim} simulated values of the ratio within the parentheses. The estimator above applies to conditional as well as to nonconditional simulations, though the correction factor (S/S_{MC}) may vary somewhat between the two alternatives.

If the study area consists of m adjacent strata and we neglect the effect of spatial correlation between strata, the CV estimator corresponding to eq. 17 becomes

$$\hat{\text{CV}}_m = \frac{\sqrt{\sum_{i=1}^{m} \bar{b}_{si}\text{CV}_i^2 A_i^2}}{\sum_{i=1}^{m} \bar{b}_{si} A_i} \quad (18)$$

where A_i is the area of stratum i, $\bar{b}_{si}$ is the mean of observed densities in stratum i, and CV_i is calculated for each stratum separately by applying eq. 17.

A considerable improvement of the method can be obtained if the standardized density obtained by dividing each individual density observation with the stratum expectation value follows a common distribution and the standardized variogram γ_z is independent of stratum, or even better, independent of survey (time) as well. The CV estimator in eq. 18 can then be expressed as follows:

$$\hat{\text{CV}}_m = \hat{\text{std}}\left(\sum_{i=1}^{m} \bar{b}_{si} A_i \Big/ \sum_{i=1}^{m} \bar{b}_{gi} A_i\right)(S/S_{\text{MC}}) \quad (19)$$

where a common correction factor (S/S_{MC}) is calculated for the entire study area, and the terms $\bar{b}_{si}$ and $\bar{b}_{gi}$ are the simulated estimates and true densities in stratum i. In this case, within-stratum spatial correlations might be taken into account, and far more observation pairs will be available for the empirical variogram. This is demonstrated in the shrimp case study to follow.

Results

Sample population model

A rather linear relationship independent of year and stratum was found between the logarithmic value of the strata means, $\ln(\bar{b}_i)$, and the strata sampling standard deviations, $\ln(S_i)$, with a slope β close to one (Fig. 4). In addition, a smooth shape of the relative frequency distribution of the 1069 standardized density values (observed density divided by empirical stratum mean) appeared where a fitted Weibull distribution gave a good fit (Fig. 5). A standard χ^2 test based on the fitted distribution (the bins from $z = 3.2$ to $z = 5$ were lumped together) resulted in an estimated significance value (p value) of $\hat{P}_W = 0.45$. In the further simulations, the Weibull distribution was therefore applied as a parametric sample distribution, along with the empirical standardized distribution when applying reversed bootstrap, as common sample distributions of standardized densities for all strata and years.

Normalized variogram

The normalized empirical variograms were based on the normal-transformed values of the standardized densities year by year, treating the entire study area as one stratum. No apparent anisotropy was seen from the directional variograms. Isotropic annual variograms were calculated applying eq. 9 with a lag resolution (dh) of 20 n.mi. At the first lag, all distances between 0 and 30 n.mi. were included, 0 exclusive. All variograms appeared to have the same concave shape with a horizontal asymptote (Fig. 6, thin lines), and their average was calculated by using weights proportional to the number of observation pairs for each year at each lag (Fig. 6, ●). In addition, the variogram parameters were estimated by applying a modified version of eq. 10, accumulating 5 × 5 succeeding discrete lags to obtain a sufficient number of pairs at each lag (Fig. 6, ○). Each sample location was approximated to the nearest simulation grid node. The results were $\hat{r}$ = 77.4 n.mi., NU = 0.406, and SI = 1.07, and the resulting variogram is shown by the broken line in Fig. 6. Based on 5000 simulations and eq. 10, the corresponding empirical standard deviations were 4.5 n.mi., 0.063, and 0.032, respectively, and considerably smaller bias estimates. For mathematical convenience, the values r = 75 n.mi and NU = 0.4 were used in the simulations of random realizations of the process, which were close to the bias corrected estimates 0.39 n.mi., and 75.1 n.mi., respectively. Further, SI = 1 was used for the sill parameter, which is the appropriate value in $N(0,1)$ space.

The summation terms (before squaring) in the weighted least square sum defined by eq. 10 appeared to be rather independent, with a constant variance independent of lag (Fig. 7) and no apparent trends. A scatter plot of the normal-transformed observations with sampling nodes 20 n.mi. apart showed no apparent deviation from a binormal distribution, with a correlation coefficient given by the model (Fig. 8). Applying the latter (ρ = 0.37), a 95% ellipse was constructed, and the number of observations outside the ellipse did not deviate significantly (5% test level) from the binormal hypothesis. The independent empirical estimate of the nugget parameter based on the normal-transformed values of the standardized 115 observation pairs with $h = 0$ was 0.37, i.e., rather close to the nugget estimate when the observations at lag $h = 0$ were excluded. Thus several model-supporting features were seen from the data.

Fig. 4. Empirical stratum means vs. stratum standard deviations on a log–log scale. The fitted curve has slope equal to one, which is equivalent to a proportional relationship.

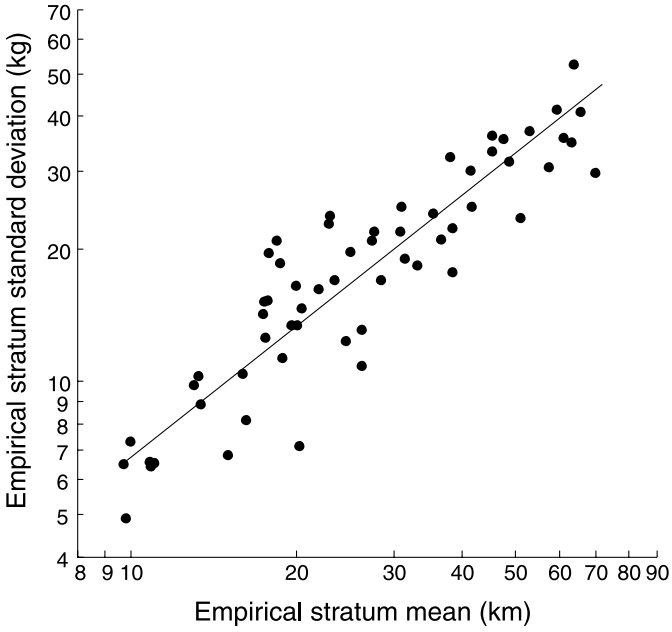

Correction factor S/S_{MC}

The correction factor S/S_{MC} based on 5000 nonconditional simulations was 1.089 when applying the Weibull distribution fit and 1.083 when applying reversed bootstrap. These close values were seen as a support to both approaches. For the conditional simulations, a slightly smaller correction factor S/S_{MC} = 1.074 was found based on reversed bootstrap.

Note that the factors do not contain the finite area effect alone, but also the finite sample size effect resulting from the use of empirical means instead of unknown expectation values in the establishment of the standardized empirical sample distribution. To separate the finite sample size effect, simulations were conducted with NU = 1 (no spatial structure), because in this case, the finite area effect disappears. The result was a scaling factor S/S_{MC} = 1.035, with a negligible difference between conditional and nonconditional simulations.

Abundance precision

A 5035 × 5035 covariance matrix $\mathbf{C}(\mathbf{x}_g,\mathbf{x}_g)$ for the process in normal-transformed space was calculated based on all of the 5035 4 and 2 n.mi. nodes in the simulation grid and the previously established variogram. The nonconditional random normal $N(0,1)$ realizations for the entire study area at each grid node were generated applying eq. 12, and the conditional simulations were generated by use of eq. 16. These were transformed to standardized biomass densities by applying the empirical distribution of standardized densities as well as the Weibull fitted distribution and then were multiplied by the empirical strata means. The simulated CV was calculated by applying eq. 17. The Cholesky decomposition

Fig. 5. Empirical sample distribution of 1069 biomass values from 1992–2002 divided by their empirical stratum mean at the year at which they were sampled, with fitted Weibull distribution.

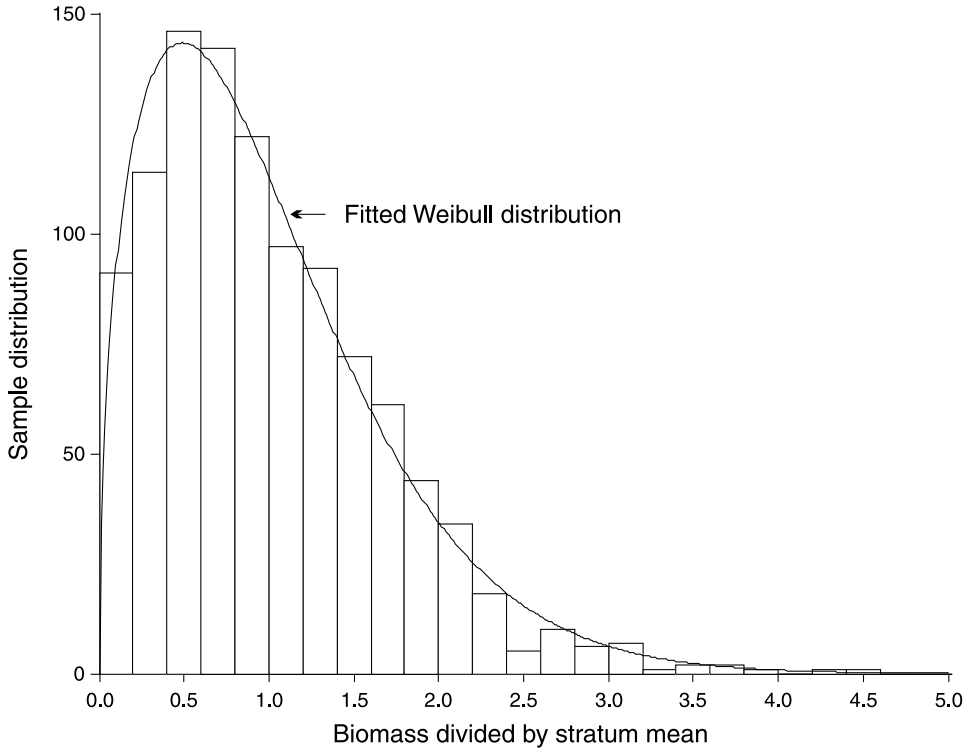

Fig. 6. Shrimp (*Pandalus borealis*) variograms based on Φ-transformed, standardized biomass values. Thin lines illustrate annual empirical variograms for each of 11 years (20 nautical mile (n.mi.) resolution), and solid circles (●) indicate average over years. Smaller, open circles (○) indicate more discrete empirical estimates, accumulating 5 × 5 succeeding distinct lags. The dotted line illustrates the fitted theoretical variogram with estimated parameters.

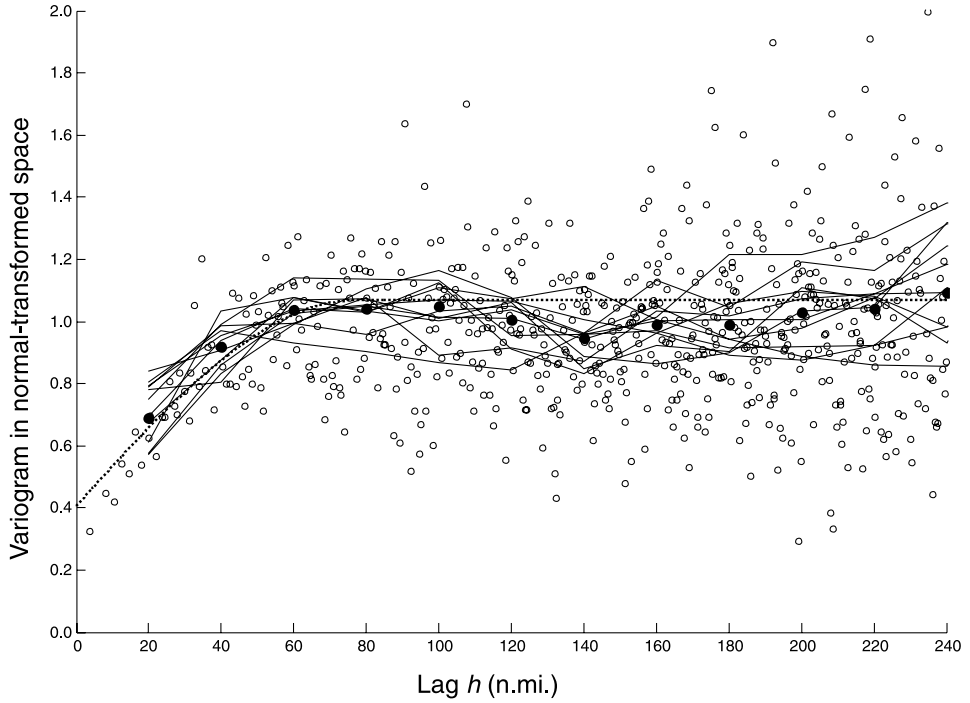

of $\mathbf{C}(\mathbf{x}_g,\mathbf{x}_g)$ with Matlab 5.3 took 36 s of CPU time on a PC with 2.2 GHz processor and 768 Mb RAM, with similar computing times required for the other analyses.

Based on 5000 reversed bootstrap simulations, the average CV value over years was 6.4%, based on regular sampling and conditional simulations (Table 1). For nonconditional

Fig. 7. (*a*) Summation terms $\ln(\hat{\gamma}_Z / \gamma_Z) n_d$ minimizing weighted square sum used to define estimates for NU, SI, and *r*, see eq. 10, as a function of lag, h_d. (*b*) Random normal plot of independent normal variables with mean and variance equal to series in (*a*). Nautical mile, n.mi.

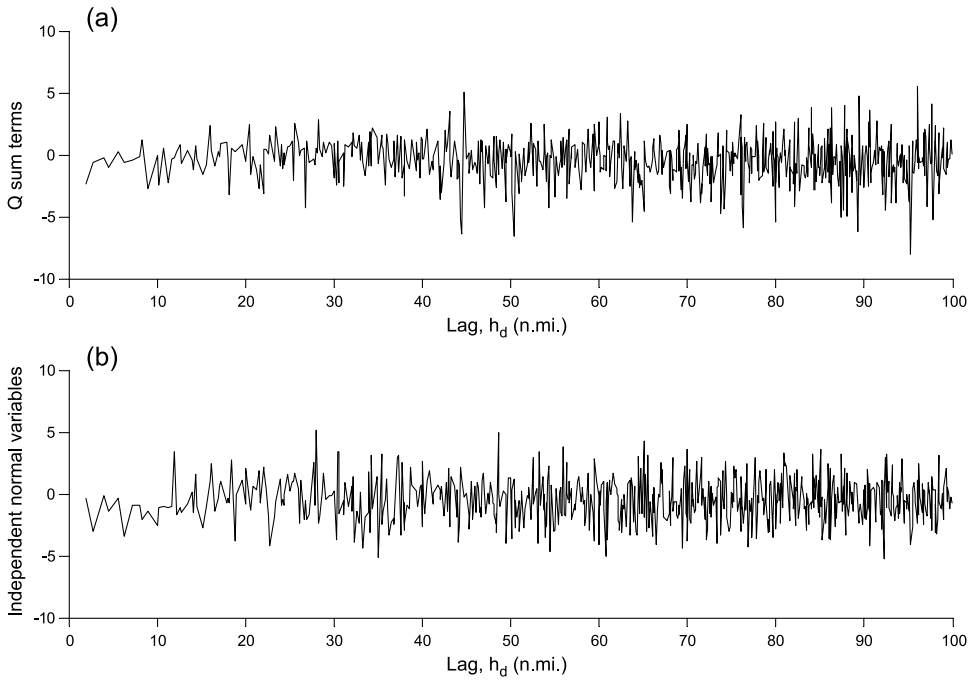

simulations, the corresponding average was 7.4% for the reversed bootstrap simulations and 7.2% for the Weibull simulations. The same marginal difference between the reversed bootstrap and Weibull approaches was seen for nonconditional simulations and random sampling, i.e., with random locations within each stratum (average CV = 8.2% and 8.0%, respectively). These results indicate that an appropriate CV estimator is found by the conditional simulation approach and that the regular design in this case is substantially better than the random design. On average, the conditional CV estimator is also considerably smaller than the wrongly calculated CV based on data alone and neglecting spatial correlations. An exception is 1996 when a rather dramatic increase in CV is seen (CV = 7.8%), whereas a rather small CV is calculated assuming uncorrelated data (CV = 6.0%). This clearly indicates the need to take spatial correlations into account in this case.

The CV was also simulated for different values of NU (n_{sim} = 2000, *r* = 75 n.mi.) based on perfect regular sampling by applying the 118 idealized sampling grid nodes instead of real locations and with strata means proportional to the average strata means over years (μ = 10*k*, 15*k*, 20*k*, 10*k*, 30*k*, and 15*k* for strata A, B, C, D, E, and F, respectively, with *k* an arbitrary scaling constant). For NU = 0.4, the CV based on random locations was 30% larger than that based on regular sampling, i.e., comparable to the relative difference between random and regular results from the Barents Sea data. The CV dependence on NU for the idealized regular case appeared to be rather linear, with a CV value of 3.1% for NU = 0 (Fig. 9), i.e., about half of the CV obtained with random sampling. Again a negligible difference is seen between the Weibull simulations and reversed bootstrap, also regarding the CV for random sampling. More interestingly, a negligible difference between conditional (Fig. 9, heavy broken line) and nonconditional simulations is seen as well. For random locations, we also see that the results based on only the sample nodes (Fig. 9, ● and +) are similar, but more stable, than the results obtained by use of all simulation grid nodes (Fig. 9, solid and dotted lines).

Fig. 8. Scatter plot of normal-transformed values of densities with sampling node locations 20 nautical miles (n.mi.) apart. The dotted line indicates model-based 95% ellipse.

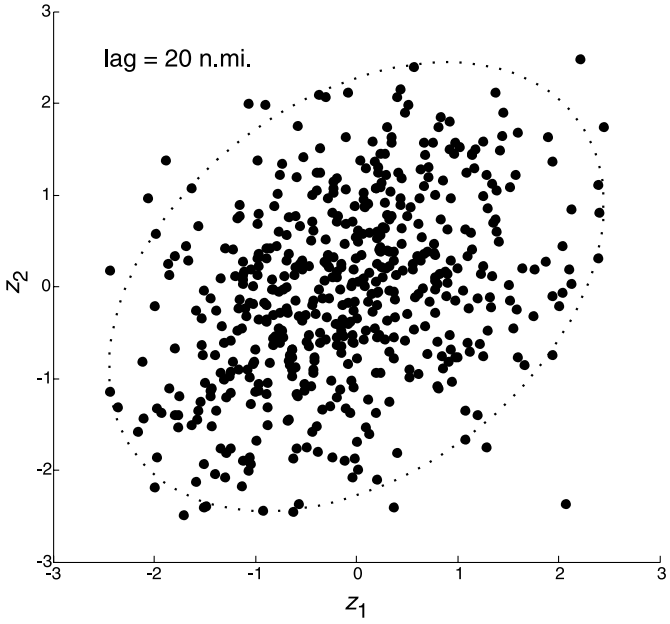

Table 1. Comparison of coefficient of variation (CV) values for the Barents Sea data by parametric (Weibull) and nonparametric (bootstrap) approach, conditional and nonconditional simulations, and by the actual sampling sites (approximately regular grid) and random sample locations.

	CV, regular sampling, nonconditional simulation (%)		CV, random sampling, nonconditional simulation (%)		CV, regular sampling, conditional simulation (%)	CV, spatial correlation neglected (%)
Year	Weibull	Bootstrap	Weibull	Bootstrap	Bootstrap	Data only
1992	5.7	5.9	7.1	7.1	5.3	5.6
1993	6.8	7.0	8.0	8.0	6.4	6.2
1994	6.8	6.8	8.1	8.5	6.3	8.6
1995	6.1	6.5	7.8	8.2	5.9	9.4
1996	10.6	10.6	9.9	9.8	7.8	6.0
1997	7.3	7.4	8.1	8.6	6.7	9.3
1998	8.4	8.5	8.0	8.1	7.7	8.0
1999	6.0	6.4	8.0	8.2	5.9	8.2
2000	6.3	6.3	7.5	8.1	5.9	7.2
2001	6.8	7.3	8.4	8.6	6.4	6.2
2002	7.9	8.3	7.3	7.5	6.3	7.9
Average	7.2	7.4	8.0	8.2	6.4	7.5

Note: The far-right column contains CV results when spatial correlation is neglected.

Fig. 9. Simulated abundance (%) coefficient of variation (CV; 2000 simulations) for different values of NU in the normalized variogram and with r = 75 nautical miles. Heavy broken line illustrates results based on conditional simulations, the others are based on nonconditional simulations. Lower curves are based on regular sampling with sampling locations at the 118 idealized 20 nautical mile sampling grid nodes. Upper curves are based on 118 random sampling locations with the same number of values within each stratum as for regular sampling. Solid lines are based on reversed bootstrap; dotted lines are based on Weibull fit. Solid circles (●; reversed bootstrap) and plus signs (+; Weibull fit) indicate random location results based only on sampling nodes.

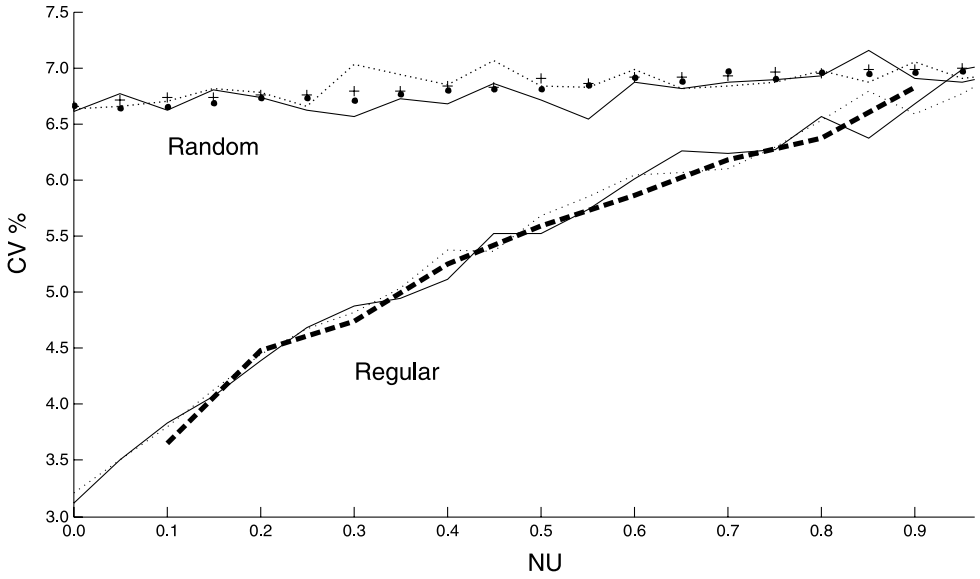

Discussion

The dramatic difference in CV between conditional and nonconditional simulations for 1996 is explained by the ice coverage in the stratum where shrimp were most abundant, preventing evenly distributed samples over the area. The extension of the sampled subarea was about the same as the extension of the noncovered subarea and comparable to the correlation length, r. Using nonconditional simulations, we expect several realizations with substantially larger abundance in the sampled subarea than in the noncovered subarea, and vice versa, which will increase the simulated CV. By conditional simulations, however, the abundance difference between the two subareas will remain more constant, as a consequence of the constraint that the simulations are conditional on the actual observations of density.

A large difference in CV between conditional and nonconditional simulations was also seen for the 2002 data. In this case, some clusters of very close sampling points (2 n.mi. grid) were chosen to study spatial correlations at a fine scale. One of these clusters consisted of nine points in a square in the most abundant stratum (Fig. 1, stratum E). Using nonconditional simulations, sometimes the mean density in a cluster will be considerably larger than the true stra-

tum average, and sometimes considerably smaller. This will increase the simulated CV. However, using conditional simulations, the difference between the cluster average and the true stratum average will remain more constant.

The CV differences between conditional and nonconditional simulation for the regular design clearly illustrate that the CV is sensitive to deviations from an idealized grid, because no apparent difference is seen in the latter case. This also provides a plausible explanation for why the change in CV among methods (regular vs. random) does not correspond well over time. The general change in CV between years is also due to annual variations in sample size and the relative importance (i.e., abundance of shrimp) of each stratum.

As expected, the CV results for random locations can be estimated by using the sampling nodes alone, ignoring the other grid nodes, as verified by the simulations. In this case, the CV can be simply estimated from data without simulations, ignoring possible spatial correlations. Similar results would come from data in a sufficiently ideal regular grid. Thus data from a regular grid can be used to estimate the CV that would be obtained by random locations, independent of a spatial structure or not, without the need for simulations. In practice, however, an idealized sampling design will often not be used, and in these cases, simulations are useful for "almost random" situations.

The assumption of a second-order homogenous process is crucial for this method to be appropriate. An objection to the homogeneity assumption in the shrimp case study is related to border effects. The irregular border of the study area is closely related to the depth contours, because the shrimp abundance is negligible in shallow areas. It is therefore natural to question if the spatial structure will be different close to the border contrary to the centre of the area. No such behaviour is apparent at first glance, probably because of slowly changing depths. The effect of the border enclosing the study area is a task for further studies.

The assumption of having homogenous conditions within each stratum with different average densities in the different strata is obviously a simplification, because this implicitly assumes a very steep gradient at the strata borders. In practice, density will vary more smoothly between strata, equivalent to the presence of local trends. These trends may influence the concave shape of the variogram at small lags. To examine this, a "nonergodic" covariance and corresponding variogram can be constructed (Isaaks and Srivastava 1988) consisting of the covariance of the "head" and "tail" observation for each observation pair at each lag. A preliminary analysis applied to the shrimp data using the northernmost location as the head location and the southernmost location as the tail location revealed that the concave shape of the variogram was modified only slightly.

The term "process distribution" was introduced as a term for the distribution of densities to be used in the simulations of random process realizations. Applying an appropriate scaling (variance adjustment) of the sampling distribution of densities provided a reasonable estimate of the process distribution. This idea could be extended to also take into account properties other than the variance, which can vary from the process to the sampling distribution. If, for example, the Weibull distribution appears to give a good fit to the sampling distribution, as well as to the simulated sampling distribution provided by applying the sampling distribution as process distribution, then the Weibull parameters in the latter can be adjusted. In this manner, not only the variance difference, but also the difference in shape between the process and sampling distributions, can be taken into account. To examine if such an approach is reasonable, an extensive and hierarchical simulation scheme could be applied, in some analogy to double bootstrap or calibration (Efron and Tibshirani 1993; Davison and Hinkley 1997).

Acknowledgements

Petter Abrahamsen at the Norwegian Computing Centre in Oslo, Professor Nils Lid Hjort at the University of Oslo, and Professor Henning Omre at the Technical University of Norway in Trondheim provided great help with clarifying discussions and encouraging comments. Peter Corceron at the Institute of Marine Research helped improve the clarity of the writing. The referees also contributed substantially to the improvement of the paper. This research was directly connected to the shrimp assessment financed by the Norwegian Fisheries Department. We thank the scientific staff and crews of R/V *Jan Mayen* for assistance with fieldwork over many years.

References

Aschan, M., and Sunnanå, K. 1997. Evaluation of the Norwegian Shrimp Surveys conducted in the Barents Sea and the Svalbard area 1980–1997. ICES CM 1997/Y:07.

Beardwood, J., Halton, J.H., and Hammersley, J.M. 1959. The shortest path through many points. Proc. Cambridge Philos. Soc. **55**: 299–327.

Chilès, J.P., and Delfiner, P. 1999. Geostatistics. Modeling spatial uncertainty. John Wiley & Sons, Inc., New York.

Christofides, N., and Eilon, S. 1969. Expected distances in distribution problems. Operations Res. Quart. **20**(4): 437–443.

Cochran, W.G. 1977. Sampling techniques. 3rd ed. John Wiley & Sons, Inc., New York.

Cressie, N.A.C. 1993. Statistics for spatial data. John Wiley & Sons, Inc., New York.

Davison, A.C., and Hinkley, D.V. 1997. Bootstrap methods and their application. Cambridge University Press, Cambridge.

Efron, B., and Tibshirani, R.J. 1993. An introduction to the bootstrap. Chapman & Hall, London.

Harbitz, A., and Lindstrøm, U. 2001. Stochastic spatial analysis of marine resources with application to minke whales (*Balaenoptera acutorosatrata*) foraging: a synoptic case study from the southern Barents Sea. Sarsia, **86**: 485–501.

Harbitz, A., Aschan, M., and Sunnanå, K. 1998. Optimal effort allocation in stratified, large area trawl surveys, with application to shrimp surveys in the Barents Sea. Fish. Res. **37**: 107–113.

Isaaks, E.H., and Srivastava, R.M. 1988. Spatial continuity measures for probabilistic and deterministic geostatistics. Math. Geol. **20**(4).

Kern, J.W., and Coyle, K.O. 2000. Global block kriging to estimate biomass from acoustic surveys for zooplankton in the western Aleutian Islands. Can. J. Fish. Aquat. Sci. **57**: 2112–2121.

Loeng, H. 1991. Features of the physical oceanographic conditions in the Barents Sea. Polar Res. **10**: 5–18.

Mardia, K.V., Kent, J.T., and Bibby, J.M. 1992. Multivariate analysis. Academic Press, London.

Petitgas, P. 1993. Geostatistics for fish stock assesments: a review and an acoustic application. ICES J. Mar. Sci. **50**: 285–98.
Ripley, B.D. 1987. Stochastic simulation. John Wiley & Sons, Inc., New York.
Rivoirard, J., Simmonds, J., Foote, K.G., Fernandes, P., and Bez, N. 2000. Geostatistics for estimating fish abundance. Blackwell Science, London.
Thompson, S.K. 1992. Sampling. John Wiley & Sons, Inc., New York.
Thompson, S.K., and Seber, G.A.F. 1996. Adaptive sampling. John Wiley & Sons, Inc., New York.

Appendix A. Notations.

- A area
- B abundance, e.g., biomass in study area
- b density, e.g., tonnes per square nautical mile
- $\bar{b}_s$ mean empirical density based on data or simulations at sample nodes
- $\bar{b}_g$ mean simulated density based on simulations in all grid nodes
- $\bar{b}_i$ empirical stratum mean
- c subscript for conditional
- $\mathbf{C}$ covariance matrix $\mathbf{C} = \{c_{jk}\}$ in $N(0,1)$ space with SI = 1
- $\mathbf{C}_0$ covariance matrix with NU = 0 and SI = 1
- c_{jk} element in $\mathbf{C}$, $c_{jk} = \text{cov}(b(\mathbf{x}_j), b(\mathbf{x}_k))$
- $\mathbf{D}$ matrix with property $\mathbf{DD}^T = \mathbf{C}$, e.g., a Cholesky decomposition of $\mathbf{C}$
- CV coefficient of variation (standard deviation divided by mean)
- F cumulative sample distribution
- g subscript for grid
- $\mathbf{h}$ vector lag, i.e., vector distance between two observation sites
- h lag, scalar distance between two observation sites, $h = |\mathbf{h}|$
- i index for stratum, $i = 1,\ldots, m$
- iid abbreviation for independent and identically distributed
- j and k index for spatial location
- il composed index for location l in stratum i
- m number of strata
- MC abbreviation for Monte Carlo
- n number of samples
- nc subscript for nonconditional
- N number of grid nodes in simulation grid
- n.mi. nautical mile
- n_{sim} number of simulations
- NU nugget parameter in variogram
- q catchability
- r correlation length, parameter in variogram
- Q weighted sum of squares to estimate variogram parameters
- s subscript for sampling
- S sample standard deviation
- S_{MC} estimated sampling standard deviation applying S as true process standard deviation
- SI sill parameter in variogram
- R rank
- rnd abbreviation for random
- $\mathbf{x}$ spatial coordinate vector in two-dimensional Cartesian coordinate system, $\mathbf{x} = (x,y)$
- x spatial coordinate in Cartesian coordinate system
- y spatial coordinate in Cartesian coordinate system
- z normal $N(0,1)$ variable
- Φ^{-1} inverse cumulative $N(0,1)$ distribution
- γ variogram
- μ expected average density in defined area
- σ standard deviation in process distribution

Appendix B. Simulation procedure for conditional simulation.

1. Transform from data, $b_1,\ldots,b_n$, to normal $N(0,1)$ variables $z_1,\ldots,z_n$, e.g.,

$$z_j = \Phi^{-1}(\text{rank}(b_j)/(n+1)), \quad j = 1,\ldots,n$$

2. Calculate empirical variogram $\hat{\gamma}_Z(h)$ based on $z_1,\ldots,z_n$ and fit theoretical variogram, e.g.,

$$\gamma_Z(h) = \begin{cases} \text{NU} + (\text{SI} - \text{NU})(1.5(h/r) - 0.5(h/r)^3), & h \le r \\ \text{SI}, & h > r \end{cases}$$

3. Calculate $N \times N$ grid correlation matrix $\mathbf{C}_g = \mathbf{C}(\mathbf{x}_g,\mathbf{x}_g) = \{c_{jk}\}$ with SI = 1:

$$c_{jk} = 1 - \gamma_z(h_{jk};\ \text{SI} = 1), \quad j \ne k,\ j,k = 1,\ldots,N$$

$$c_{jj} = 1, \quad j = 1,\ldots,N$$

$$h_{jk} = |\mathbf{x}_{gj} - \mathbf{x}_{gk}|$$

4. Calculate $n \times n$ sampling correlation matrix $\mathbf{C}_s = \mathbf{C}(\mathbf{x}_s,\mathbf{x}_s) = \{c_{jk}\}$ as in point 3, but now with $h_{jk} = |\mathbf{x}_{sj} - \mathbf{x}_{sk}|$ and with N replaced by n.
5. Calculate $N \times n$ cross covariance matrix $\mathbf{C}_0 = \mathbf{C}_0(\mathbf{x}_g,\mathbf{x}_s)$, but now with

$$c_{jk} = 1 - \gamma_z(h_{jk};\ \text{NU} = 0,\ \text{SI} = 1),$$

$$h_{jk} = |\mathbf{x}_{gj} - \mathbf{x}_{sk}|, \quad j = 1,\ldots,N,\ k = 1,\ldots,n$$

6. Calculate $N \times N$ conditional grid covariance matrix $\mathbf{C}_c$ and corresponding $N \times N$ decomposition matrix $\mathbf{D}_c$:

$$\mathbf{C}_c = \mathbf{C}_g - (1 - \text{NU})^2\mathbf{C}_0\mathbf{C}_s^{-1}\mathbf{C}_0^T$$

$$\mathbf{D}_c\mathbf{D}_c^T = \mathbf{C}_c$$

7. Calculate random conditional simulations $\mathbf{z}_c(\mathbf{x}_g) = (z_{c1},\ldots,z_{cN})^T$ in all grid nodes:

$$\mathbf{z}_c(\mathbf{x}_g) = (1 - \text{NU})\mathbf{C}_0\mathbf{D}_s^{-1}\mathbf{z}_s + \mathbf{D}_c\mathbf{z}_{iid}$$

where $\mathbf{z}_{iid}$ is a $N \times 1$ vector of independent $N(0,1)$variables.
8. Backtransform to observation space by, e.g., reversed bootstrap:

$$R = \text{int}(n\Phi(z_{cj})) + 1;$$

$$b_{cj} = b_{(R_j)}, \quad j = 1,\ldots,N$$

where $b_{(R_j)}$ is the R_jth lowest observed density value.
9. Repeat steps 7–9 n_{sim} times and calculate CV = std($\bar{b}_s/\bar{b}_g$), i.e., the standard deviation of the n_{sim} values of the ratio between "observed" and "true" density.
10. Multiply CV with correction factor S/S_{MC}, where S is the empirical sample standard deviation and S_{MC} is the average sample standard deviation from the simulations.